

## Effects of fire intensity on carbon dioxide exchange in an arctic dry heath tundra

Wenyi Xu<sup>a,b,\*</sup> , Per Lennart Ambus<sup>a</sup>

<sup>a</sup> Department of Soil and Environment, Swedish University of Agricultural Sciences, Lennart Hjelm's väg 9, 756 51 Uppsala, Sweden

<sup>b</sup> Department of Geosciences and Natural Resource Management, University of Copenhagen, Øster Voldgade 10, 1350 Copenhagen, Denmark

### ARTICLE INFO

#### Keywords:

Greenland  
Tundra fire  
Net ecosystem change  
Gross ecosystem production  
Ecosystem respiration  
Vegetation recovery

### ABSTRACT

The frequency and intensity of wildfires in the Arctic has been increasing due to climate change. However, little is known about the effects of fire intensity on carbon dioxide (CO<sub>2</sub>) exchange in arctic tundra ecosystems. To investigate this, we conducted an experimental fire with different burn intensities (low intensity, high intensity, and unburned control) and measured surface daytime CO<sub>2</sub> fluxes over four growing seasons in a dry heath tundra in West Greenland. We found that post-fire soil temperatures and moisture increased with increasing fire intensity, by up to 2.2 °C and 18 vol%, respectively. Fire had no effects on soil microbial biomass independent of intensity. The high-intensity fire increased soil nitrate concentrations only immediately after the fire. The ecosystem shifted from a net CO<sub>2</sub> sink to a net CO<sub>2</sub> source immediately after the fire, due to the reduced gross ecosystem production. One year after the fire, the low-intensity burned plots became a net CO<sub>2</sub> sink, while the high-intensity burned plots remained a net CO<sub>2</sub> source throughout the study period. This suggests that the time needed for the ecosystem to become a net CO<sub>2</sub> sink increases with fire intensity. Fire intensity had no effect on soil respiration, but the high-intensity fire significantly reduced ecosystem respiration (ER) rates one and three years after the fire. This suggests that decreased ER was mainly driven by the reduced aboveground plant respiration. Over four growing seasons after the high-intensity fire, cumulated post-fire C losses exceeded the C losses during the fire. Thus, it is essential to consider the long-term C losses following fire to improve understanding of wildfire impacts on arctic tundra C dynamics. Overall, this study highlights that high-intensity fires prolong the duration of burned areas as a net CO<sub>2</sub> source, leading to increased post-fire CO<sub>2</sub> emissions, when compared to low-intensity fires.

### 1. Introduction

In the Arctic, air temperature has increased by 0.75 °C during the past decade, far outpacing the global average (Post et al., 2019). During this period, due to particularly drier and warmer summers, the frequency and intensity of wildfire has also increased in the arctic tundra regions (Lewis et al., 2019; McCarty et al., 2020), such as Alaska, Siberia and Greenland (Rocha and Shaver, 2011a; Hu et al., 2015; Evangeliou et al., 2019; Talucci et al., 2022). Wildfires can start with a lightning strike or a human-made spark. The spread and duration of fire are regulated by many factors, such as fuel availability, wind speed and moisture (Pereira et al., 2018). Fires in the arctic dry tundra are usually fast-moving, with limited downward heat transfer, due to low aboveground biomass and windy conditions (Walker et al., 2020; Hermesdorf et al., 2022).

The arctic region is a globally important C storage; accounting for approximately 50 % of the global soil C, due to low decomposition rates under cold and poorly-drained conditions (Hugelius et al., 2014; Schuur et al., 2018). Tundra fires have profound consequences for ecosystem biogeochemical cycles (Knicker, 2007; Bowman et al., 2009), through the combustion of plant biomass and soil organic matter (SOM), and the changes in physical, chemical and biological soil environment conditions (Mack et al., 2011; Bret-Harte et al., 2013; Ludwig et al., 2018). Hence, increasing occurrence and extent of wildfires with climate change in the Arctic can cause substantial C losses to the atmosphere, significantly altering the global C budget, and leading to a positive climate feedback.

Fire intensity represents the energy released during different phases of a fire. Various metrics, including reaction intensity, fireline intensity, temperature, heating duration, heat load, and radiant energy, serve

\* Corresponding author.

E-mail address: [wenyi.xu@slu.se](mailto:wenyi.xu@slu.se) (W. Xu).

<https://doi.org/10.1016/j.agrformet.2024.110362>

Received 11 November 2023; Received in revised form 10 October 2024; Accepted 8 December 2024

Available online 20 December 2024

0168-1923/© 2024 The Authors. Published by Elsevier B.V. This is an open access article under the CC BY license (<http://creativecommons.org/licenses/by/4.0/>).

distinct purposes in quantifying this phenomenon (Keeley, 2009). Fire intensity affects the amount of vegetation and SOM consumed by fire and thus the magnitude of changes in soil microclimate, soil nutrient availability, and carbon dioxide (CO<sub>2</sub>) fluxes following fire (McCarty et al., 2021). Soil temperatures can increase with increasing fire intensity due to larger losses of insulating layers of vegetation and SOM, and reductions in surface albedo arising from the darker surface (Kennard and Gholz, 2001; Certini, 2005). In the permafrost-affected region, fire-induced increases in soil temperatures may lead to thawing of previously frozen soil horizons and thereby destabilize deeper storages of soil C and N (Brown et al., 2015; Ribeiro-Kumara et al., 2020). Pyrogenic C (char) is formed when organic matter, such as plant material, is exposed to high temperatures during a fire, but the combustion process is not complete. The extent of char formation is often dependent on the fire intensity, with higher-intensity fires typically producing more char. Fire may elevate soil moisture content by enhancing soil water retention due to the incorporation and infiltration of char/ash into soils (Stoof et al., 2010; Potter and Hugny, 2020), or by ceasing the evapotranspiration due to the loss of vegetation (Montes-Helu et al., 2009). Soil nutrient availability post fire can increase with increasing fire intensity due to the increasing amount of char/ash produced by fire and consequently the release of more nutrients, and greater microbial mineralization activities at higher soil temperatures (Kennard and Gholz, 2001; Pereira et al., 2012).

Due to increasing vegetation mortality and reductions in above-ground or root biomass, plant photosynthetic activity and respiration decreases and net ecosystem CO<sub>2</sub> emission increases with increasing fire intensity, which turns the ecosystem into a bigger net CO<sub>2</sub> source (Kelly et al., 2021). Thus, the time needed for vegetation to recover and ecosystems to turn from a net CO<sub>2</sub> source into a net CO<sub>2</sub> sink following fire depends largely on fire intensity (Hermesdorf et al., 2022). Soil respiration includes the CO<sub>2</sub> released by soil microorganisms (heterotrophic respiration) and plant roots (autotrophic respiration) within the soil. Ecosystem respiration accounts for all CO<sub>2</sub> emissions from various ecosystem components, extending beyond the soil to include above-ground plant biomass within the ecosystem. Fire can stimulate soil microbial respiration through increasing soil temperatures and nutrient availability (Certini, 2005; Dooley and Treseder, 2012; Abdalla et al., 2016). On the other hand, microbial respiration may decline after fire, particularly after a high-intensity fire, due to the reductions in soil C quantity and quality and shifts in the size, composition and activity of microbial community (Day et al., 2019; Adkins et al., 2020). Fire intensity can exert a direct influence on plant roots by exposing them to thermal stress. High-intensity fires can inflict damage or mortality on plant roots, subsequently reducing autotrophic respiration rates (Zhou et al., 2023). The pyrogenic C has highly recalcitrant chemical structures and is largely resistant to microbial decomposition, and can act as a long-term C sink, potentially sequestering C and reducing CO<sub>2</sub> emissions (Knicker, 2007). A growing number of studies have been investigating the effects of fire intensity on soil CO<sub>2</sub> fluxes in boreal forest ecosystems (Morishita et al., 2014; Koster et al., 2018; Ludwig et al., 2018; Kelly et al., 2021), but still little is known about effects of fire intensity in arctic tundra ecosystems. Moreover, most studies have focused on CO<sub>2</sub> effluxes from soils post fire, not considering effects of recovering vegetation and changes in CO<sub>2</sub> fluxes associated with above-ground plants, and thus fire impacts on whole ecosystem CO<sub>2</sub> exchange are even sparser.

In this study, we conducted an experimental fire with three intensities (i.e., low intensity, high intensity and unburned control) in a dry heath tundra ecosystem in West Greenland. We assessed the impacts of fire intensity on soil microclimate, soil nutrient availability and ecosystem CO<sub>2</sub> exchange over four growing seasons after the fire. Thus, the underlining hypotheses are that (I) post-fire soil temperatures and moisture as well as soil nutrient availability increase with increasing fire intensity due to increasing char/ash deposition; (II) the time needed for the burned ecosystem to turn into a net CO<sub>2</sub> sink increases with

increasing fire intensity due to more vegetation removal; and (III) ecosystem respiration declines with increasing fire intensity due to decreasing soil microbial and plant respiration.

## 2. Material and methods

### 2.1. Site description

The study is located at Blåsedalen Valley (69°16N, 53°27W), on the south of Disko Island, West Greenland. This valley is in the transition zone between the Low and High Arctic and has a typical Low Arctic climate (Borggaard and Elberling, 2007). Based on meteorological data (1991–2017) from the nearby Arctic station, the annual mean air temperature was  $-3 \pm 1.8$  °C, with monthly mean temperature ranging from 8 °C in July to  $-14$  °C in March. The annual mean precipitation (1991–2017) was  $418 \pm 131$  mm, of which 34 % was snowfall. The area is within a discontinuous permafrost zone and the maximum active layer is estimated to be more than 3 m deep. The mineral soil with basaltic rock fragments in the study area is covered by a thin organic layer (ca. 5 cm). The annual mean soil temperature at 5 cm depth is  $-1.9$  °C and frozen soil conditions prevail from October to late May (D'Imperio et al., 2018). The vegetation is typical for a dry heath tundra, dominated by low shrubs (height < 10 cm) of deciduous and dwarf birch (*Betula nana* L.), cowberry (*Vaccinium uliginosum* L.), and gray willow (*Salix glauca* L.) and evergreen (Arctic bell-heather (*Cassiope tetragona* (L.) D. Don)) shrubs, with a mixture of lichens (*Cetraria islandica* (L.) Ach. and *Stereocaulon paschale* spp.) and mosses (*Tomentypnum nitens* (Hedw.) Loeske and *Aulacomnium turgidum* (Wahlenb.) Schwägr.) covering the ground.

### 2.2. Experimental setup and design

In July 2019, the study site was established on a gentle northeast facing slope (5.7° inclination). The experimental design includes three treatments (plot size 2 × 2 m), i.e. Control (C), low-intensity fire (L), and high-intensity fire (H), randomly organized in five replicate blocks (block size 2 × 6 m) (Fig. 1). The choice of this design reflects a compromise between resource constraints and logistical feasibility, in line with similar approaches in numerous other studies conducted in comparable environments (Virkkala et al., 2018). The experimental fire was made on July 30th, 2019. The low-intensity fire was achieved by using a butane-gas burner deployed for 5 min per plot, while the high-intensity fire was deployed over 20 min per plot. The 5 or 20 min were chosen after a test burning in an adjacent dry heath area to mimic the duration of natural fires in that area (Xu et al., 2021, 2022a). After 20 min of fire aboveground vegetation biomass was completely burned away (high-intensity) whereas after 5 min (low-intensity) the burn pattern was more heterogeneous leaving unburned or scorched patches of cryptogams and some stems of shrubs yet without green leaves. A heat load index (i.e., the accumulated depth-specific temperature values recorded at 1-min intervals during 40 min from the onset of the fire) was calculated to indicate the duration of heating by a fire, which depended on the quantity of fuel consumed (Burrows, 1999). The low-intensity fire had a heat load of 285 °C minutes at the top 0–2 cm soil (maximum temperature of 357 °C) and 168 °C minutes at 5 cm soil depth (maximum temperature of 18 °C). For the high-intensity fire, the heat load was 505 °C minutes at the top 0–2 cm soil (maximum temperature of 396 °C) and 214 °C minutes at 5 cm soil depth (maximum temperature of 204 °C). In this study, soil temperatures and heat load were the two primary metrics for quantifying fire intensities during these two burning durations.

### 2.3. Carbon dioxide flux measurement

Two weeks prior to the fire, stainless steel collars (21 × 21 × 10 cm) were installed to 5 cm soil depth at each plot. Collars were mounted in the central part of the plot, or at least 0.5 m from the plot boundary if conditions allowed due to the occurrence of larger stones (Fig. 1).

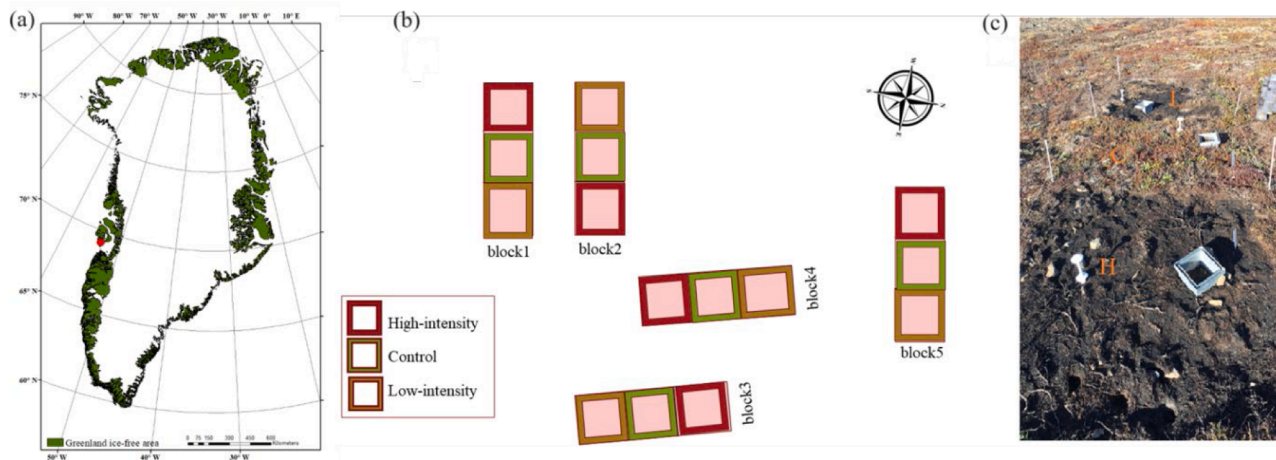


**Fig. 1.** A map of Greenland (a). The location of study site is indicated by a red dot. Experimental design overview of the tundra fire experiment in Blåsedalen, Disko Island, West Greenland (b). A picture of the control (C), low-intensity (L) and high-intensity (H) burned plots (c). (For interpretation of the references to colour in this figure legend, the reader is referred to the web version of this article.)

Surface daytime  $\text{CO}_2$  flux was measured using the static chamber technique (Denmead, 2008). The plexiglass chambers ( $21 \times 21 \times 19.5$  cm) were mounted in the collars, and water was added to the grooves atop the collars to establish a gas-tight seal between chamber enclosure and the outside atmosphere. The measurements of daytime  $\text{CO}_2$  fluxes were conducted five times in 2019 (from August 1st to September 6th), seven times in 2020 (from June 23rd to August 22nd), and twice in both 2021 (July 1st and August 20th) and 2022 (July 28th and August 13th). Each plot was measured twice by using a  $\text{CO}_2$  infrared gas analyzer (EGM-5, PP System, Amesbury, USA). The first measurement was taken under light conditions with a transparent chamber to establish net ecosystem exchange (NEE). The second measurement was conducted under dark conditions with a chamber covered by a black cloth to establish ecosystem respiration (ER). The ecosystem respiration data suggested a probable increase in soil respiration (SR) following the fire. Therefore, we conducted measurements of SR to examine the changes in soil respiration after the fire. The measurements of SR were conducted three times (August 20th, 2021, July 28th and August 13th, 2022). Soil respiration was measured in each plot by using a soil respiration chamber (SRC-2) connected to the EGM-5 analyzer. The SRC-2 fits to soil collars made of PVC cylinders (10 cm diameter and 7 cm height) and pushed 5 cm into the soil. The cylinders were pre-installed at locations adjacent to the metal collars, ensuring there was no aboveground vegetation within the 10-cm ring. All the gas measurements were taken between 11:00 and 14:00 to reduce diurnal variations of fluxes.

For all measurements (NEE, ER, SR) the changes in  $\text{CO}_2$  concentrations inside the flux chamber were analyzed and logged at a 1 s sampling frequency for 5 min. Because our chamber measurement data showed a stronger fit with linear regression better (higher  $R^2$ ) than non-linear regression models, we calculated  $\text{CO}_2$  fluxes by fitting a linear regression ( $p < 0.05$ ,  $R^2 > 0.9$ ) to changes in  $\text{CO}_2$  concentrations over time. Gross ecosystem production (GEP) was calculated by subtracting ER from NEE rates. Given that NEE was not significantly correlated with soil temperatures, and other data (e.g. time series aboveground biomass) were missing for model stimulation/upscaling, the post-fire C losses were calculated as the sum of the seasonal-integrated  $\text{CO}_2$ -C fluxes from 2019 to 2022. The seasonal-integrated  $\text{CO}_2$ -C fluxes (from June to early September) were estimated as the sum of the  $\text{CO}_2$ -C fluxes integrated over the number of days between two consecutive campaigns (D'Imperio et al., 2017; St Pierre et al., 2019). To estimate C losses during fire, the aboveground biomass and litter were collected at the nearby area, then air-dried, and shipped to the laboratory in Copenhagen. The C losses during the high-intensity fire were estimated as the C losses of the aboveground biomass and litter after the three thermal

conversion processes, i.e. torrefaction ( $250^\circ\text{C}$ , anoxic atmosphere), pyrolysis ( $550^\circ\text{C}$ , anoxic atmosphere), and combustion ( $550^\circ\text{C}$ , ambient atmosphere). This is assumed to be representative for thermal and oxygen conditions during an arctic wildfire when vegetation biomass has been completely burned away (Pluchon et al., 2015; Safdari et al., 2018).

Along with gas flux measurements, soil temperature and soil moisture were manually recorded in triplicates within each plot next to the collar. Soil temperature and soil volumetric moisture (%vol) at 5 cm depth were measured with a HI93503 (Hanna Instruments, Woonsocket, RI, USA) and a ML2X Theta Probe coupled to a HH2 Moisture Meter (Delta-T Devices, Cambridge, UK), respectively. The albedo and normalized difference vegetation index (NDVI) was measured in triplicates one meter above the surface within each plot by using an albedo (ISM 400 Solar Power Meter, RS Components, Copenhagen, DK) and a SKR 10 sensor (Skye instruments, Powys, UK), respectively.

#### 2.4. Soil temperature and soil moisture

Soil temperatures at 0–2 cm and 5 cm depths during the burning process were measured in three of five blocks, using a RS-PRO 1384 datalogger with Type K Thermocouples (RS Components, Copenhagen, DK). Long-term soil temperature and moisture TOMST loggers (TMS-4, TOMST, Prague, Czech Republic) were installed on July 30th, 2019. The loggers measured and recorded soil temperatures and moisture at 6 cm soil depth at 15 min intervals.

#### 2.5. Soil sampling and analysis

On July 31st, 2019, August 5th, 2020 and July 29th, 2022, 2 or 3 replicate soil samples per plot were collected in the top 0–5 cm soil by using a 20-mm-diameter auger. The exact number of samples varied according to the occurrence of stones in the plots. The replicate samples were subsequently mixed thoroughly into one composite sample. Coarse roots and stones were removed by hand, and soil moisture was calculated from oven drying weight loss ( $65^\circ\text{C}$ , 48 h). For total C and N analyses, 20–30 mg of oven dried and finely ground soil was placed in tin cups, folded and analyzed by elemental analysis (CE1110, Thermo Electron, Milan, Italy). Soil extractions were made by suspending field moist soil in deionized water (10 g soil; 50 mL water), shaking for 1 hour at room temperature and then filtrated through  $2.7\ \mu\text{m}$  membrane filter (Whatman GF/D). To quantify soil microbial biomass C (MBC) and N (MBN), the soil was fumigated by vacuum incubation using chloroform ( $\text{CHCl}_3$ ) for one day before extraction. Filtrates were kept frozen until

analyzed for ammonium ( $\text{NH}_4^+\text{-N}$ ), nitrate ( $\text{NO}_3^-\text{-N}$ ) and phosphate ( $\text{PO}_4^{3-}\text{-P}$ ) using flow-injection analysis (Tecator 5000 FIAStar, Höganäs, Sweden). Soil dissolved organic C (DOC) and total dissolved N (TDN) from the filtered extracts were measured using a TOC-TN analyzer (Shimadzu, Kyoto, Japan). Dissolved organic N (DON) was calculated as the difference between TDN and dissolved inorganic N ( $\text{NO}_3^-\text{-N} + \text{NH}_4^+\text{-N}$ ). MBC and MBN were calculated as the difference between fumigated and non-fumigated data.

## 2.6. Ex-situ soil $\text{CO}_2$ flux measurement

Ex-situ soil incubation was conducted as a supplementary experiment to investigate how soil microbial respiration changed after the fire. On August 8th, 2021, soil samples were collected in the top 0–3.5 cm depth from all the plots, with a 6-cm-diameter steel cylinder. The intact soil cores (top 0–3.5 cm,  $99 \text{ cm}^3$ ) were kept under frozen conditions ( $-18^\circ\text{C}$ ) and shipped to a laboratory in Copenhagen, Denmark. The frozen samples were thawed stepwise, first to  $-8^\circ\text{C}$  for one day and then to  $0^\circ\text{C}$  for one day prior to use. The soil cores were transferred into 365-mL jars (with screw lids), placed in an adjustable freezer at a temperature of  $10^\circ\text{C}$  and equilibrated for 48 h. To make incubation conditions comparable in terms of soil moisture content and aeration, all the soil cores were gently wetted with 40 mL water and drained for 24 h at  $10^\circ\text{C}$  prior to the measurement. The used incubation temperature was based on in-situ soil temperatures in top 5-cm depth from late July to early August. The soil  $\text{CO}_2$  flux was measured three times at a 2-day interval. The jars were closed air-tightly during each measurement and connected in a closed loop mode to the  $\text{CO}_2$  infrared gas analyzer. The changes in headspace  $\text{CO}_2$  concentrations were analyzed and recorded at a 1 s sampling frequency for 5 min. The  $\text{CO}_2$  fluxes were calculated by fitting a linear regression ( $p < 0.05$ ,  $R^2 > 0.9$ ) to changes in  $\text{CO}_2$  concentrations over time.

## 2.7. Aboveground vegetation biomass

To estimate aboveground vegetation biomass, all biomass was collected by cutting at soil surface from a representative area of  $20 \times 20$  cm within each plot. The area was chosen to be representative for both the vegetation at each plot in general but also for that inside the collar. The collected biomass samples were dried at  $65^\circ\text{C}$  for 48 h and then weighed.

## 2.8. Statistics

Prior to analysis, the data were checked for normal distribution and homogeneity of variance by inspecting the QQ-plots as well as by using Shapiro-Wilk normality test or Levene's test. If necessary, the data were subsequently log- or square-root- transformed to meet assumptions. We tested effects of fire intensity on variations in  $\text{CO}_2$  fluxes, soil properties, albedo, NDVI and aboveground vegetation biomass by using one-way ANOVA. The test was carried out separately for each campaign (or across all campaigns) using a linear mixed effects model with the lme4 and car packages (Bates et al., 2015; Fox and Weisberg, 2019). In the test, the replicate block was specified as a random factor accounting for spatial variations within the site. Post-hoc pairwise comparisons between levels of all significant factors were then conducted using the emmeans package. Statistical significance is based on  $p \leq 0.05$ . All analyses above were performed using R software v. 4.2.1 (Team, 2021).

## 3. Results

### 3.1. Meteorological observations

Meteorological data showed contrasting air temperature and liquid precipitation between the four growing seasons (June to September 2019–2022) (Fig. 2). The growing season 2019 had the highest mean air temperature ( $8.7^\circ\text{C}$ ) and the lowest seasonal accumulated liquid precipitation (111 mm), while the growing season 2022 was the coldest and wettest, with a mean air temperature of  $5.7^\circ\text{C}$  and an accumulated liquid precipitation of 212 mm (Fig. 2).

### 3.2. Albedo, NDVI and aboveground vegetation biomass

Both low- and high-intensity burning significantly decreased the albedo measured two days (August 1st, 2019) after the fire ( $p < 0.01$ ); the high-intensity significantly more than the low-intensity ( $p < 0.01$ ; Table 1). One (August 22nd, 2020) and two years (August 20th, 2021) after the fire, high-intensity burning still had significantly lower albedo values as compared with control plots ( $p = 0.02$  and  $p = 0.04$ , respectively), while low-intensity fire had no significant effects (Table 1). Three years after the fire, the albedo did not significantly vary among fire intensities (Table 1).

The NDVI was significantly affected by fire intensity, with the lowest values in high-intensity burned plots (H), intermediates in low-intensity

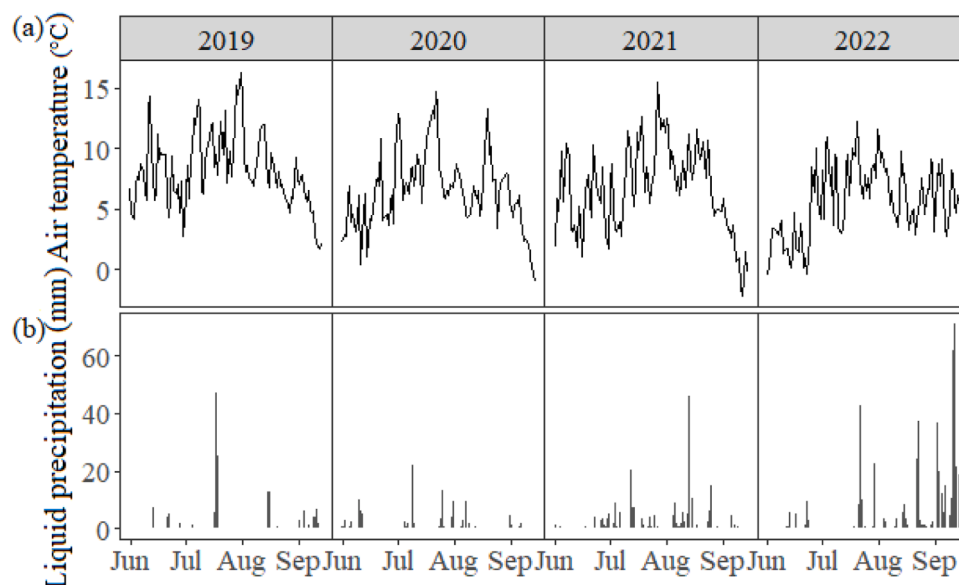


Fig. 2. Mean daily air temperature (a) and liquid precipitation (b) from June to September in 2019–2022 in Blåsedalen, Disko Island, West Greenland.

**Table 1**

Effects of fire intensity on albedo, normalized difference vegetation index (NDVI), aboveground vegetation biomass, and C losses during and post fire in Blåsedalen, Disko Island, West Greenland.

		C	L	H	
Albedo	August 1st, 2019	0.20 ±0.01 <sup>c</sup>	0.14 ±0.01 <sup>b</sup>	0.09 ±0.00 <sup>a</sup>	
	August 22th, 2020	0.27 ±0.01 <sup>b</sup>	0.24 ±0.01 <sup>ab</sup>	0.23 ±0.00 <sup>a</sup>	
	August 20th, 2021	0.27 ±0.01 <sup>b</sup>	0.26 ±0.01 <sup>ab</sup>	0.24 ±0.01 <sup>a</sup>	
	July 28th, 2022	0.18±0.01	0.21±0.02	0.19 ±0.01	
	August 13th, 2022	0.21±0.01	0.21±0.01	0.20 ±0.01	
	NDVI	August 22th, 2020	0.44 ±0.02 <sup>b</sup>	0.42 ±0.02 <sup>ab</sup>	0.39 ±0.02 <sup>a</sup>
		August 20th, 2021	0.38 ±0.01 <sup>b</sup>	0.34 ±0.02 <sup>a</sup>	0.33 ±0.01 <sup>a</sup>
		July 28th, 2022	0.66 ±0.02 <sup>c</sup>	0.45 ±0.04 <sup>b</sup>	0.30 ±0.04 <sup>a</sup>
		Aboveground vegetation biomass (g m <sup>-2</sup> )	August 1105.4 ±	333.5 ±	158.8 ±
		14th, 2022	88.3 <sup>b</sup>	140.5 <sup>a</sup>	101.8 <sup>a</sup>
C losses during fire (g m <sup>-2</sup> )	0	N.D.	408.6 ±		
C losses post fire (g m <sup>-2</sup> )	-273.8 ±	109.1 ±	228.7 ±		
	64.5 <sup>a</sup>	50.3 <sup>b</sup>	33.8 <sup>c</sup>		

Numbers show mean (±SE) of replicate blocks ( $n = 5$ ). Control (C), low-intensity (L) and high intensity (H). Lowercase letters indicate significant differences ( $p \leq 0.05$ ) between fire intensities within each date (one-way ANOVA). N.D., no data due to difficulty in estimating incompletely burned biomass.

burned plots (L), and the highest in control plots (C; Table 1).

Nearly three years after the fire, aboveground vegetation biomass has not recovered to pre-fire levels, and two-fold higher aboveground biomass was observed at low-intensity burned plots (L) compared with high-intensity burned plots (H,  $p = 0.07$ ; Table 1).

### 3.3. Soil properties

Basic physical, chemical and biological soil properties after low- and high-intensity fire are shown in Figs. 3 and 4. The low-intensity fire significantly increased daily mean soil temperature at 6 cm depth (maximum increase of 1.4 °C) during each of the three growing seasons (June to September 2019–2021), although to a lower extent compared with high-intensity fire (maximum increase of 2.2 °C) (Fig. 3). There were also significant increases in soil moisture at 0–6 cm depth due to the fire during the three growing seasons (by 2–12 vol% and 6–18 vol% for the low- and high-intensity burning, respectively) ( $p < 0.01$ ; Fig. 3).

As observed one day after the fire (July 31st, 2019), bulk soil C, N, C/N ratio and pH had not been affected (at 0–5 cm depth) by the fire intensity and averaged (at control plots)  $8.1 \pm 2.5\%$ ,  $0.5 \pm 0.1\%$ ,  $18.7 \pm 1.9$  and  $6.22 \pm 0.06$ , respectively (Table S1).

In contrast to bulk soil characteristics, observations one day after the fire revealed a significant and positive effect of high-intensity fire on soil  $\text{NO}_3\text{-N}$  concentrations. Concentrations of DOC,  $\text{NH}_4\text{-N}$  and  $\text{PO}_4\text{-P}$  were generally higher in high-intensity burned plots as compared to controls, however, the effects were not significant (Fig. 4). The effects had disappeared about one (August 5th, 2020) and two years after the fire (July 29th, 2021; Fig. 4). Microbial biomass C and N was not significantly affected by the fire intensity and averaged (at control plots)  $1880 \pm 443$  mg C kg<sup>-1</sup> and  $43 \pm 11$  mg N kg<sup>-1</sup>, respectively (Fig. 4).

### 3.4. Ecosystem CO<sub>2</sub> exchange

Net ecosystem exchange (NEE) rates (at control plots) were dominantly negative over the study period, indicating that the studied ecosystem was generally a net CO<sub>2</sub> sink. The NEE was significantly affected by fire intensity, ranging from  $-164.6 \pm 58.9$  at control plots to  $182.2 \pm 41.3$  mg CO<sub>2</sub> m<sup>-2</sup> h<sup>-1</sup> at high-intensity burned plots (Fig. 5a). The low-intensity and high-intensity burning increased net ecosystem CO<sub>2</sub> losses immediately after the fire, with mean NEE rates of  $123.2 \pm 17.4$  and  $144.1 \pm 17.1$  mg CO<sub>2</sub> m<sup>-2</sup> h<sup>-1</sup>, respectively, in growing season

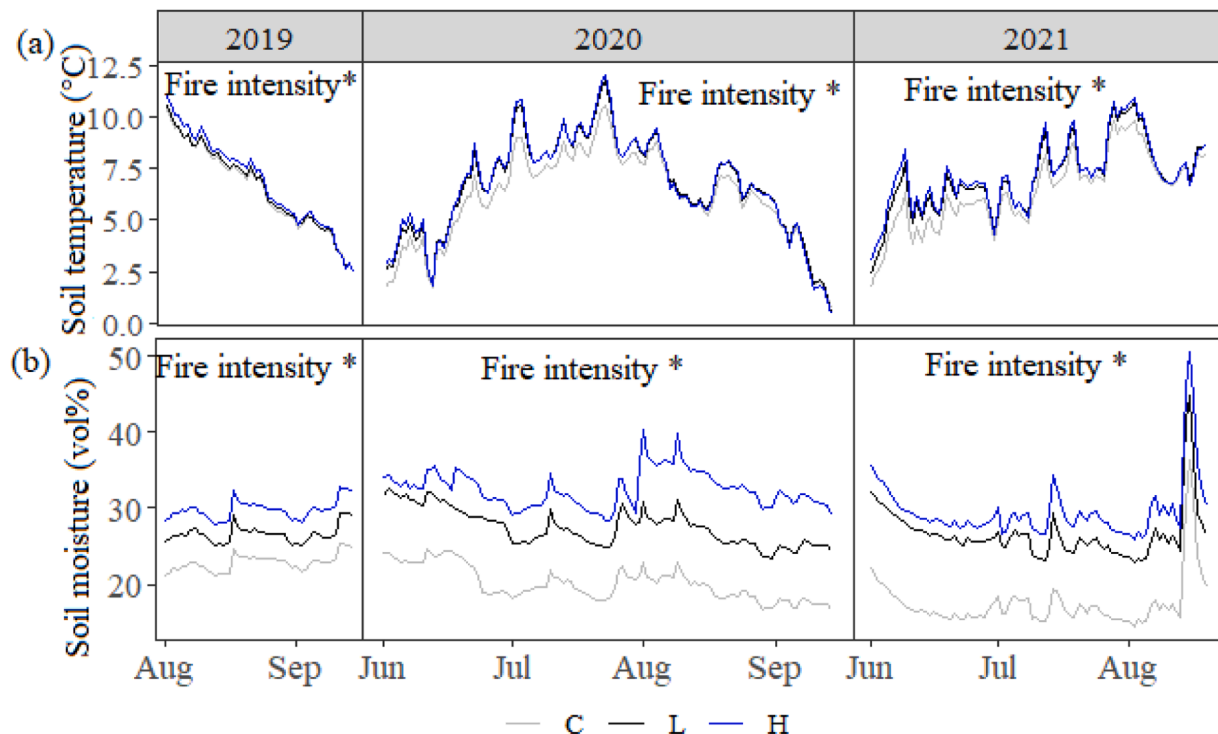


**Fig. 3.** Effects of fire intensity on soil temperature (a) and volumetric water content (b) from June to September in 2019–2021 in Blåsedalen, Disko Island, West Greenland. Control (C), low-intensity (L) and high intensity (H). Significant effects of fire intensity within each year (one-way ANOVA) are shown as  $*p \leq 0.05$ .

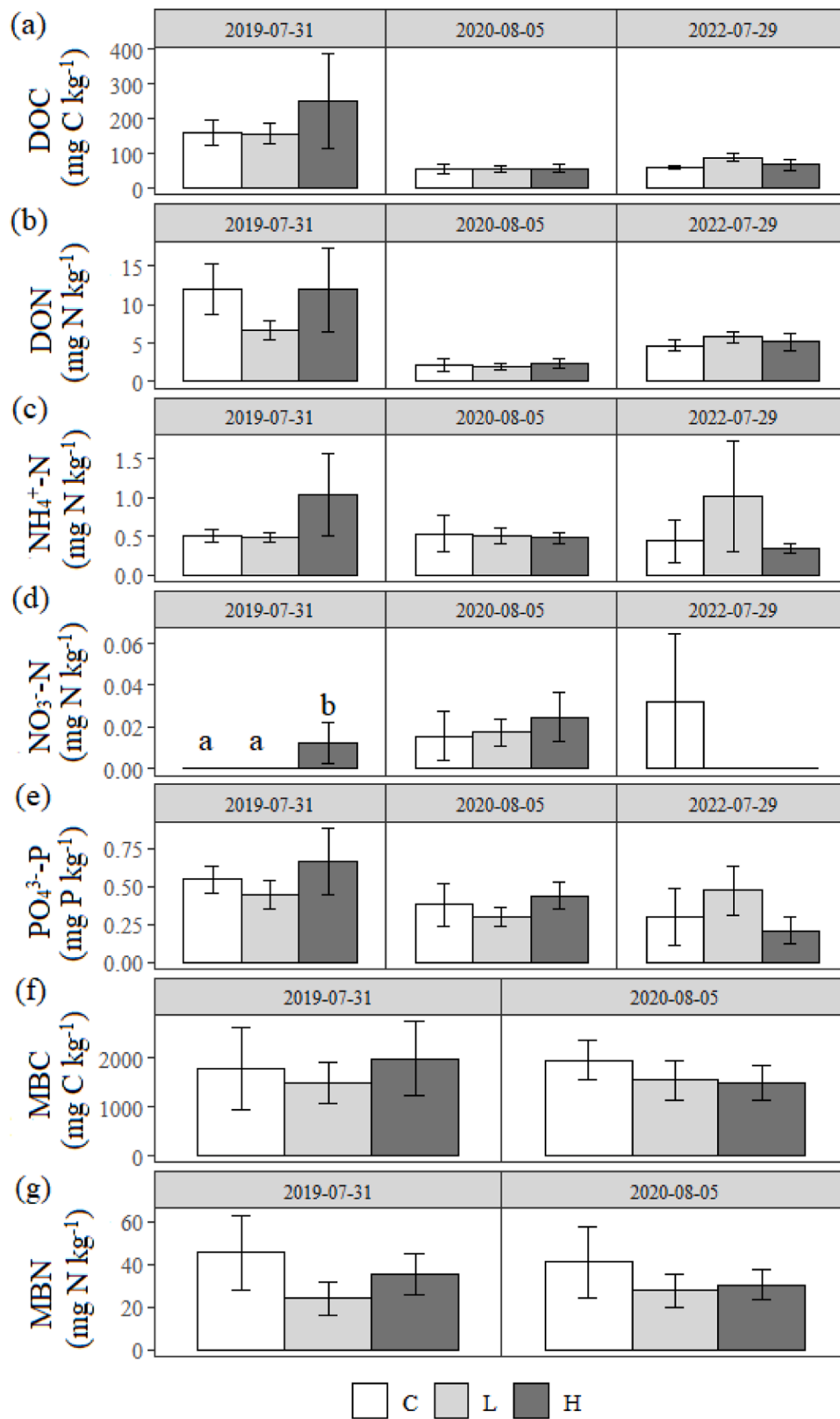


**Fig. 4.** Effects of fire intensity on soil (a) DOC, (b) DON, (c) NH<sub>4</sub><sup>+</sup>-N, (d) NO<sub>3</sub><sup>-</sup>-N, (e) PO<sub>4</sub><sup>3-</sup>-P, (f) microbial biomass C (MBC), and (g) microbial biomass N (MBN) in Blæsedalen, Disko Island, West Greenland. Control (C), low-intensity (L) and high intensity (H). Bars show mean ( $\pm$ SE) of replicate blocks ( $n = 5$ ). Lowercase letters ( $p \leq 0.05$ ) indicate significant differences between fire intensities within each campaign (one-way ANOVA).

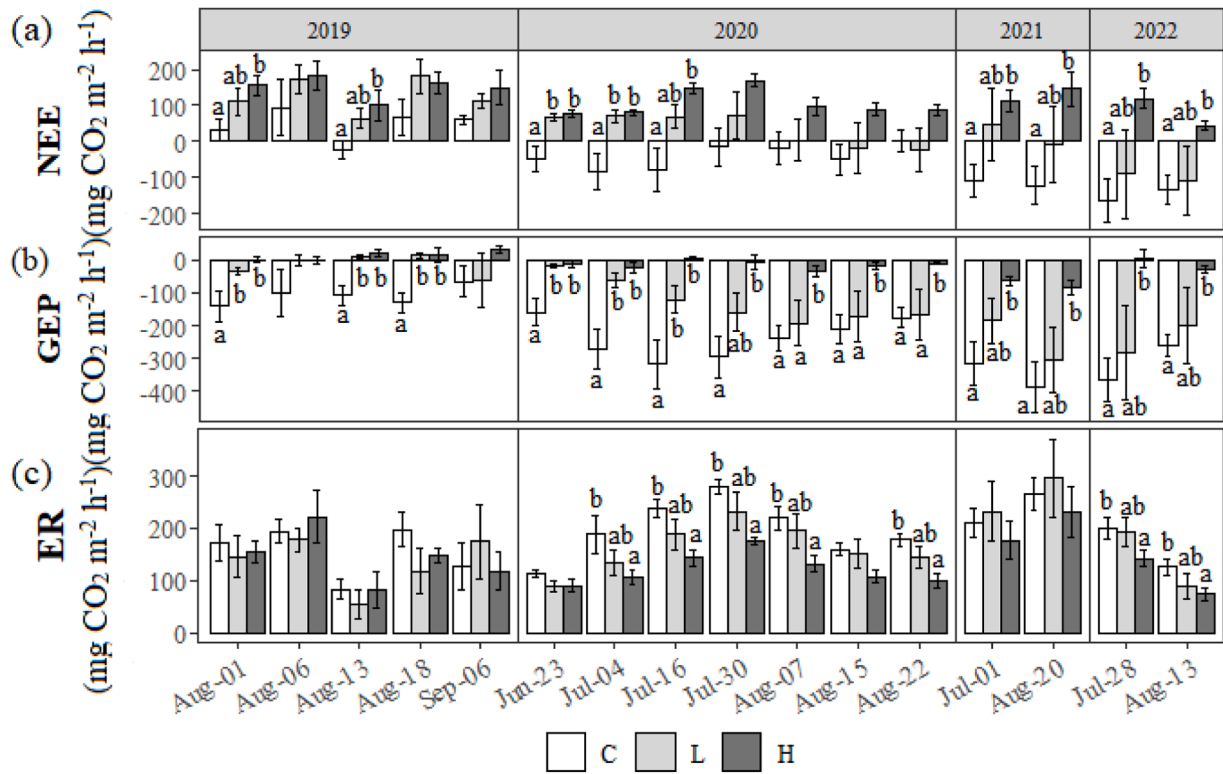


**Fig. 5.** Effects of fire intensity on net ecosystem exchange (a), gross ecosystem production (b), and ecosystem respiration (c) in growing seasons 2019–2022 in Blåsedalen, Disko Island, West Greenland. Control (C), low-intensity (L) and high intensity (H). Bars show mean ( $\pm$ SE) of replicate blocks ( $n = 5$ ). Lowercase letters ( $p \leq 0.05$ ) indicate significant differences between fire intensities within each campaign (one-way ANOVA).

2019 (Fig. 5a). The low-intensity burned plots also had significant impacts on NEE rates at the first three campaigns in growing season 2020 ( $p < 0.05$ ), while afterwards NEE rates did not differ significantly between control and low-intensity burned plots (Fig. 5a). The stimulating effect of high-intensity fire on CO<sub>2</sub> losses in general lasted for the entire study period (Fig. 5a). The low-intensity burned plots did not turn into a net CO<sub>2</sub> sink until one year after the fire (after July 30th, 2020), while high-intensity burned plots remained net CO<sub>2</sub> sources in growing seasons 2020–2022, indicated by consistently positive NEE rates (Fig. 4a).

The burning (both low- and high-intensity) significantly decreased gross ecosystem production (GEP) rates as compared with control plots two, 14 and 19 days after the fire ( $p \leq 0.05$ ), indicating reduced photosynthetic activities immediately after the fire (Fig. 5b). The low-intensity burned plots exhibited lower GEP rates than control plots at the first three campaigns in the growing season 2020 ( $p < 0.01$ ), while afterwards (one year after the fire) low-intensity burned plots had more negative rates and did not significantly differ from control plots (Fig. 5b). In contrast, the high-intensity burned plots showed consistently lower GEP rates compared with control plots in the growing seasons 2020–2022 (Fig. 5b). Moreover, there were significantly higher GEP rates in low-intensity burned plots observed at the last three campaigns in growing season 2020, when compared with high-intensity burned plots ( $p < 0.05$ ; Fig. 5b).

Immediately after the fire (2019), there were no significant effects of fire intensity on ecosystem respiration (ER) rates (Fig. 5c). However, one (2020) and three years (2022) after the fire, the ER rates varied significantly among fire intensity, ranging from  $73.4 \pm 13.0$  to  $295.7 \pm 74.6$  mg CO<sub>2</sub> m<sup>-2</sup> h<sup>-1</sup> (Fig. 5c). One and three years after the fire, the high-intensity burning significantly reduced ER rates ( $p \leq 0.05$ ), while low-intensity fire had no significant effects on ER rates (Fig. 5c).

### 3.5. Soil respiration and ex-situ soil CO<sub>2</sub> production

Soil respiration (SR) rates ranged from  $13.7 \pm 5.6$  to  $78.3 \pm 24.9$  mg CO<sub>2</sub> m<sup>-2</sup> h<sup>-1</sup> and were not significantly impacted by fire intensity (Fig. 6). The ex-situ soil CO<sub>2</sub> production rates significantly differed among fire intensity, with 1.5-fold higher rates observed at high-intensity burned plots than the other two treatment plots across campaigns ( $p < 0.01$ ; Fig. S1). For each specific campaign, the high-intensity burned plots showed higher rates than control plots at campaign 1 ( $p = 0.07$ ) and low intensity burned plots at campaigns 2–3 ( $p \leq 0.05$ ; Fig. S1).

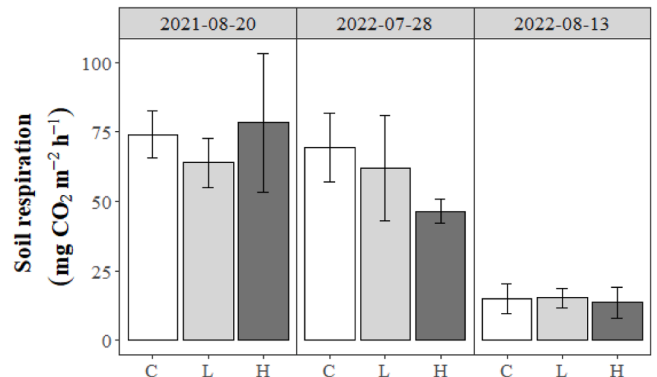


**Fig. 6.** Effects of fire intensity on soil respiration in Blåsedalen, Disko Island, West Greenland. Control (C), low-intensity (L) and high intensity (H). Bars show mean ( $\pm$ SE) of replicate blocks ( $n = 5$ ).

## 4. Discussion

### 4.1. Effects of fire intensity on soil microclimate, nutrients and microbial biomass

Both low- and high-intensity fires resulted in significant increases in post-fire soil temperatures, which can be explained by the darkened surface and consequently reduced albedo (Table 1). This is consistent with other studies on tundra wildfires, where the combustion of isolating vegetation and organic layers and the deposition of ash/char caused increases in soil temperatures (Hu et al., 2015; Bond-Lamberty et al., 2016). The high-intensity fire increased soil temperatures significantly as compared with low-intensity fire, which can be explained by the greater loss of vegetation cover and higher amount of produced ash/char, and corresponding darker surface. This is reflected by the lower NDVI and albedo following the high-intensity fire (Table 1). Soil moisture content was also significantly elevated by the high-intensity fire, and to a greater extent compared with the low-intensity fire. The removal of aboveground biomass by fire and thus reductions in evapotranspiration may lead to the increased soil moisture water content post fire (Montes-Helu et al., 2009). Moreover, the ash produced by fire has been suggested to increase soil water retention, because the incorporation or infiltration of ash into soils can fill soil pores and consequently limit infiltration rates, or water can be absorbed by the ash particles (Woods and Balfour, 2008; Stoof et al., 2010). A number of studies have reported the effect of ash on soil water retention to increase with increasing ash quantity (Woods and Balfour, 2010; Bodí et al., 2014; Lu et al., 2014). The degree of combustion and the amount of ash increase with increasing fire intensity, which could thus explain the greater magnitude of increases in soil moisture observed at high-intensity burned plots.

Immediately (one day) after the fire, soil NO<sub>3</sub>-N concentrations in near-surface layers were significantly higher at high-intensity burned than unburned plots, as also observed in other studies conducted in boreal and tundra ecosystems (Kulmala et al., 2014; Ludwig et al., 2018; Kelly et al., 2021; Klupar et al., 2021). The immediate increases in soil nutrient concentrations post fire were likely due to the decreased plant uptake (Karhu et al., 2015), the direct release of mineral N and heterocyclic N from the ash/char (Dannenmann et al., 2018; Xu et al., 2022b), and the accelerated N mineralization and nitrification activities resulting from higher soil temperatures (Caon et al., 2014; Ludwig et al., 2018). Unlike for the high-intensity fire, we did not observe an increase in soil nutrients immediately after the low-intensity fire. This could be attributed to the lower amount of produced ash/char and consequently the limited mineral and heterocyclic N release (Kennard and Gholz, 2001; Pereira et al., 2012). Further, mineral N produced via mineralization of heterocyclic N and nitrification is thus likely to be lower in the topsoil (Certini, 2005; Xu et al., 2022b). In addition, soil temperatures after the low-intensity fire increased to a lower extent compared with high-intensity fire (Fig. 2), which might not be sufficient to significantly alter the rates of microbial N-transformation processes. However, this needs to be interpreted with caution, since soil nutrient analysis immediately after the fire was only based on one soil sampling (one day post fire) and post-fire soil nutrient concentrations were reported to be very dynamic (Karhu et al., 2015; Ludwig et al., 2018), which could thus mask fire effects on soil nutrients. The lack of fire effects on nitrate availability after one and two years were expected due to a nutrient loss related to leaching, surface runoff and uptake by plants (Thomas et al., 2000; Pereira et al., 2018). Similarly, in a boreal forest, soil nutrient concentrations already declined one week after an experimental fire, and no significant effect of fire intensity on soil nutrients was observed after one year (Ludwig et al., 2018).

Burning of vegetation and soil organic layer combined with downward heat transfer may cause microbial mortality and thus declines in post-fire soil microbial biomass (Bond-Lamberty et al., 2016). The response of microbial growth and biomass to fires is largely depending

on the residence time of high temperatures rather than the maximum temperature (Lombao et al., 2020). In the current study, soil microbial biomass C and N was not significantly affected by fire intensity, which could be due to the short residence time of high temperatures during the fire. Although the top soil temperatures have been observed to rise above 200 °C during the high-intensity fire, these high soil temperatures persisted for only 2–3 min, and thus the duration of such high temperatures may not be long enough to kill microorganisms and influence soil microbial biomass. The heat load of the high-intensity fire (505 °C minutes at the top 0–2 cm soil) fell within the mid-range of the values reported by Burrows (1999) in jarrah forest fires. Wildfires in Greenlandic tundra ecosystems are predominantly caused by anthropogenic activities. They are usually fast-moving, with limited downward heat transfer, because of fuel limitations in form of low shrub biomass and shallow soil organic layers (Walker et al., 2020; Hermesdorf et al., 2022; Xu et al., 2024). This explains the short duration of high soil temperatures during the fire and thus the lack of fire effects on soil microbial biomass. The active layer depth was not affected by the fire, because fire intensity in Greenlandic tundra is much lower due to limited fuel load as compared with that in boreal forests and Alaskan tundra (Rocha and Shaver, 2011b; Morishita et al., 2014). As a result, the thermal and hydrological conditions in deep soil layers after the fire were not markedly different between burned and unburned areas.

Our observations show that the high-intensity fire increased soil temperatures and moisture content to greater extent as compared to low-intensity fire, but soil N availability was enhanced only by high-intensity fire, partly supporting our hypothesis I.

### 4.2. Effects of fire intensity on NEE

The investigated dry heath tundra ecosystem has been reported to be a net CO<sub>2</sub> sink (Ravn et al., 2020), and the experimental fire turned the burned areas into a net CO<sub>2</sub> source due to the fire-induced damage of vegetation and consequently reduced photosynthesis rates. This is consistent with observations by Rocha and Shaver (2011a) who observed that NEE reversed from a sink to a source due to the decreases in canopy photosynthesis after the Anaktuvuk River fire in Alaskan tundra. The control plots in 2019 generally acted as a net CO<sub>2</sub> source throughout the season, except on August 13. This is likely due to the timing of the measurements, which were taken two weeks after collar installation. However, the timing is not expected to have biased the relative results of the treatment effect, as all plots were uniformly affected.

One year after the fire the low-intensity burned plots have turned into a net CO<sub>2</sub> sink, while the high-intensity burned plots remained a net CO<sub>2</sub> source for at least three years. This supports our hypothesis II that the time required for the burned ecosystem to turn into a net CO<sub>2</sub> sink increases with increasing fire intensity. After a low-intensity fire, the presence of the surviving woody stems or intact belowground rhizomes allowed certain plant species to re-sprout quickly (Mack et al., 2008). In contrast, after a high-intensity fire, the complete removal of aboveground biomass and damaged or killed belowground rhizomes were unfavorable for the plant re-sprouting, slowing down the vegetation recovery rate following fire (Keeley, 2006; Hollingsworth et al., 2013). Hence, fire intensity has an impact on post-fire ecosystem CO<sub>2</sub> balance primarily by controlling the time needed for vegetation to recover from fire. Indeed, three years post fire, aboveground biomass at the low-intensity burned plots had recovered to a greater extent than high-intensity burned plots, although still lower than the unburned plots (Table S2). Similarly, Bret-Harte et al. (2013) observed that the biomass of evergreen shrubs and total living roots was significantly lower in severely burned than moderately burned areas four years after a wildfire on Alaska's North Slope. Thus, compared with low-intensity fire, high-intensity fire not only combusts more biomass or soil organic matter and releases more CO<sub>2</sub> during the fire (Kennard and Gholz, 2001; Ribeiro-Kumara et al., 2020), but also prolongs the duration of the



burned areas as a net CO<sub>2</sub> source and consequently enhances post-fire CO<sub>2</sub> losses.

Over the four growing seasons after the fire, the high-intensity burned plots exhibited a mean C loss of 502.5 g m<sup>-2</sup> (relative to the control plots), which exceeded the C losses during the fire. Considering the slow recovery of vegetation from fire in arctic tundra (Table 1), the burned areas can be a net CO<sub>2</sub> source for a longer time, causing more post-fire C losses. The post-fire C losses in arctic tundra ecosystems are of particular importance for assessing the negative effects of wildfire on C dynamics, as they can be more substantial and long-lasting than C losses during the actual fire.

Nevertheless, it's important to recognize the uncertainty due to the experimental design. One major uncertainty is the potential inability of the limited number of collars (five in this case) to adequately capture the spatial variability of CO<sub>2</sub> fluxes within the study area. Natural ecosystems often exhibit considerable spatial heterogeneity in factors influencing CO<sub>2</sub> fluxes, such as vegetation cover, soil properties, and microclimatic conditions. The choice of collar placement could introduce biases if they are not representative of the broader landscape. For instance, selecting collars in areas with higher or lower vegetation cover may skew the results, leading to inaccuracies in flux estimates. Despite the limited number of collars, the design minimizes spatial variability by strategically placing collars in the most representative areas. The study also incorporates repeated measurements across multiple years. This approach allows for the assessment of temporal patterns in CO<sub>2</sub> fluxes and helps account for short-term variability that may not be captured in single measurements. Although plants in nearby unburned areas may affect plant recovery, particularly at the boundary of the burned plots, mounting the collars at the central areas helps to minimize these effects. This allows for a more accurate representation of post-fire CO<sub>2</sub> flux dynamics associated with vegetation recovery. Given resource constraints and logistical feasibility, the choice of only five collars represents a pragmatic compromise that balances the need for robust data collection with practical considerations. Similar approaches have been employed in numerous other studies conducted in comparable environments. Future experiments could aim to expand spatial coverage by increasing the number of sampling points or utilizing advanced remote sensing techniques to capture the spatial variability of CO<sub>2</sub> fluxes more comprehensively. This would provide a more nuanced understanding of ecosystem dynamics across different landscape units.

#### 4.3. Effects of fire intensity on ER

Immediately after the fire (at the end of the growing season 2019), despite the absence of aboveground vegetation and reduced plant respiration, ER in both low- and high-intensity burned plots was comparable with unburned plots. This is in contrast to our hypothesis III that ER declines with increasing fire intensity. Observations may be attributed to an increase in soil microbial respiration that could offset the decrease in plant respiration. Several factors likely contribute to the enhanced microbial respiration, including soil nutrient availability, microclimate and organic C availability (Caon et al., 2014; Kulmala et al., 2014). Since most arctic tundra ecosystems are generally nutrient-limited, in particular at the end of the main growing season, post-fire increases in soil nutrient availability can accelerate soil microbial activity (Nowinski et al., 2008; Klupar et al., 2021). Soil temperatures and soil moisture increased after fire, especially after the high-intensity fire (Fig. 3), which may also stimulate microbial activity. The release of fine root C due to the root death after fire may enhance microbial decomposition (Díaz-Pinés et al., 2010).

Ecosystem respiration was found to be significantly lower in high-intensity burned plots compared to unburned plots one and three years after the fire. In contrast, no differences could be observed between control and low-intensity burned plots. These results could be attributed to the fact, that plant respiration declined with increasing intensity of the fire due to increasing vegetation mortality and reduced

plant biomass (Kelly et al., 2021). This is consistent with the reported decreases in annual ER rates 10 years after a high-intensity stand-replacing fire in a ponderosa pine forest (Dore et al., 2008). The lack of low-intensity fire effect on ER in the current study is consistent with the observations by Hermesdorf et al. (2022) at a nearby fire experiment. Here, they attributed the lack of changes in ER one and two years post fire to a net result of decreased plant respiration and increased microbial respiration (Hermesdorf et al., 2022). Although post-fire soil nutrient concentrations increased with increasing fire intensity (Fig. 4), these increases in nutrient availability were transient and have been reported to fade within days (Thomas et al., 2000; Pereira et al., 2018). Thus, it can be speculated that high-intensity fire immediately stimulated soil microbial respiration due to increased nutrient availability as well as increased soil temperatures and moisture, which overall counteracted the reductions in plant respiration and led to sustained respiratory CO<sub>2</sub> losses. However, one to three years post fire, the more moderate increases in microbial respiration (likely only caused by increased soil temperatures and moisture) were insufficient to offset the reductions in plant respiration, leading to declining respiratory CO<sub>2</sub> losses. In a boreal forest, Kelly et al. (2021) observed soil CO<sub>2</sub> fluxes were reduced one year after a high-intensity wildfire despite an increase of 2.7 °C in mean soil temperatures and concluded that microbial respiration was more substrate limited than temperature limited.

Two to three years after the fire, soil respiration (composed of root and microbial respiration) was unaffected by fire-intensity. This, combined with significantly increased ex-situ soil CO<sub>2</sub> production rates (an indication of microbial respiration) two years after the high-intensity fire (Fig. 6), suggests that the unaltered soil respiration can be explained as a net result of decreased root respiration (caused by vegetation damage) and enhanced soil microbial respiration. This agrees with the unaltered soil CO<sub>2</sub> fluxes four years after a wildfire in a Siberian forest, which was explained with the decreased root respiration compensated for by increased microbial decomposition (due to warmer soil) (Takakai et al., 2010). Given the fact that high-intensity fire decreased ER (Fig. 5), the lack of changes in soil respiration further suggested that the decreased ER was mainly due to the reductions in aboveground plant respiration. Therefore, it is essential to take into account both the soil CO<sub>2</sub> emissions and the uptake and emissions of CO<sub>2</sub> by plants when estimating post-fire CO<sub>2</sub> budget.

## 5. Conclusion

This study addressed the impacts of fire intensity on daytime CO<sub>2</sub> exchange and net C budget in an arctic heath tundra. Post-fire soil temperatures and soil moisture increased with increasing fire intensity. The high-intensity fire caused an immediate but transient increase in soil N availability, whereas low-intensity fire had no significant effects on soil nutrients. The combustion of aboveground vegetation and associated reductions in GEP immediately shifted the ecosystem from a net CO<sub>2</sub> sink to a net CO<sub>2</sub> source independent of fire intensity. One year after the fire, the tundra exposed to low-intense fire reversed into a net CO<sub>2</sub> sink, while the high-intensity burned tundra remained a net CO<sub>2</sub> source for the entire study period. This indicates that the time needed for the burned heath ecosystem to re-turn into a net CO<sub>2</sub> sink increases with increasing fire intensity. Fire intensity had no immediate effect on total ER, likely because the increases in microbial respiration caused by the combined effects of elevated soil temperatures and moisture and soil N availability offset the decreased plant respiration. However, one to three years after the fire, the ER, but not the SR, persisted to be reduced by the high-intensity fire, which suggests that the reduced ER was mainly linked to the decreases in aboveground plant respiration. Overall, our results stress the importance of considering post-fire C losses when estimating the impacts of wildfires on C dynamics in arctic tundra ecosystems. Furthermore, the duration of fire impacts on tundra CO<sub>2</sub> balance is extended by high-intensity fire compared to low-intensity fire. Consequently, future warmer and drier arctic summer conditions will

likely result in increased post-fire CO<sub>2</sub> losses as these conditions may also favor higher fire intensities. To gain a more comprehensive understanding of post-fire ecosystem C fluxes over time, further research on the long-term effects of high- and low-intensity wildfires in arctic tundra is needed.

### CRedit authorship contribution statement

**Wenyi Xu:** Writing – review & editing, Writing – original draft, Visualization, Investigation, Data curation. **Per Lennart Ambus:** Writing – review & editing, Supervision, Project administration, Methodology, Funding acquisition, Conceptualization.

### Declaration of competing interest

The authors declare that they have no known competing financial interests or personal relationships that could have appeared to influence the work reported in this paper.

### Acknowledgements

We gratefully acknowledge the financial support from the Danish National Research Foundation (CENPERM DNR100), and the Pioneer Center for Research in Sustainable Agricultural Futures (Land-CRAFT) funded by the Danish National Research Foundation grant number P2. We are grateful to Anders Lambæk, Lena Hermesdorf and Patrick T. N. Christensen for valuable assistance during fieldwork. We thank Arctic Station for collaboration and logistics in performing fieldwork.

### Supplementary materials

Supplementary material associated with this article can be found, in the online version, at [doi:10.1016/j.agrformet.2024.110362](https://doi.org/10.1016/j.agrformet.2024.110362).

### Data availability

Data will be made available on request.

### References

- Abdalla, K., Chivenge, P., Everson, C., Mathieu, O., Thevenot, M., Chaplot, V., 2016. Long-term annual burning of grassland increases CO<sub>2</sub> emissions from soils. *Geoderma* 282, 80–86.
- Adkins, J., Docherty, K.M., Gutknecht, J.L., Miesel, J.R., 2020. How do soil microbial communities respond to fire in the intermediate term? Investigating direct and indirect effects associated with fire occurrence and burn severity. *Sci. Total Environ.* 745, 140957.
- Bates, D., Maechler, M., Bolker, B., Walker, S., 2015. Fitting linear mixed-effects models using lme4. *J. Stat. Softw.* 67, 1–48.
- Bodí, M.B., Martín, D.A., Balfour, V.N., Santín, C., Doerr, S.H., Pereira, P., Cerdà, A., Mataix-Solera, J., 2014. Wildland fire ash: production, composition and eco-hydrogeomorphic effects. *Earth. Sci. Rev.* 130, 103–127.
- Bond-Lamberty, B., Smith, A.P., Bailey, V., 2016. Temperature and moisture effects on greenhouse gas emissions from deep active-layer boreal soils. *Biogeosciences*. 13, 6669–6681.
- Borggaard, O.K., Elberling, B., 2007. Pedological biogeochemistry. *Museum Tusulanum*.
- Bowman, D.M., Balch, J.K., Artaxo, P., Bond, W.J., Carlson, J.M., Cochrane, M.A., D'Antonio, C.M., DeFries, R.S., Doyle, J.C., Harrison, S.P., 2009. Fire in the Earth system. *Science* 324, 481–484.
- Bret-Harte, M.S., Mack, M.C., Shaver, G.R., Huebner, D.C., Johnston, M., Mojica, C.A., Pizano, C., Reiskind, J.A., 2013. The response of Arctic vegetation and soils following an unusually severe tundra fire. *Philos. Trans. R. Soc. Lond. B Biol. Sci.* 368, 20120490.
- Brown, D.R., Jorgenson, M.T., Douglas, T.A., Romanovsky, V.E., Kielland, K., Hiemstra, C., Euskirchen, E.S., Ruess, R.W., 2015. Interactive effects of wildfire and climate on permafrost degradation in Alaskan lowland forests. *J. Geophys. Res.: Biogeosci.* 120, 1619–1637.
- Burrows, N., 1999. A soil heating index for interpreting ecological impacts of jarrah forest fires. *Austral. Forest.* 62, 320–329.
- Caon, L., Vallejo, V.R., Ritsema, C.J., Geissen, V., 2014. Effects of wildfire on soil nutrients in Mediterranean ecosystems. *Earth. Sci. Rev.* 139, 47–58.
- Certini, G., 2005. Effects of fire on properties of forest soils: a review. *Oecologia* 143, 1–10.
- Dannenmann, M., Diaz-Pines, E., Kitzler, B., Karhu, K., Tejedor, J., Ambus, P., Parra, A., Sanchez-Martin, L., Resco, V., Ramirez, D.A., Povoas-Guimaraes, L., Willibald, G., Gasche, R., Zechmeister-Boltenstern, S., Kraus, D., Castaldi, S., Vallejo, A., Rubio, A., Moreno, J.M., Butterbach-Bahl, K., 2018. Postfire nitrogen balance of Mediterranean shrublands: direct combustion losses versus gaseous and leaching losses from the postfire soil mineral nitrogen flush. *Glob. Chang. Biol.* 24, 4505–4520.
- Day, N.J., Dunfield, K.E., Johnstone, J.F., Mack, M.C., Turetsky, M.R., Walker, X.J., White, A.L., Baltzer, J.L., 2019. Wildfire severity reduces richness and alters composition of soil fungal communities in boreal forests of western Canada. *Glob. Chang. Biol.* 25, 2310–2324.
- Denmead, O.T., 2008. Approaches to measuring fluxes of methane and nitrous oxide between landscapes and the atmosphere. *Plant Soil* 309, 5–24.
- Díaz-Pinés, E., Schindlbacher, A., Pfeffer, M., Jandl, R., Zechmeister-Boltenstern, S., Rubio, A., 2010. Root trenching: a useful tool to estimate autotrophic soil respiration? A case study in an Austrian mountain forest. *Eur. J. For. Res.* 129, 101–109.
- D'Imperio, L., Arndal, M.F., Nielsen, C.S., Elberling, B., Schmidt, I.K., 2018. Fast responses of root dynamics to increased snow deposition and summer air temperature in an Arctic Wetland. *Front Plant Sci.* 9, 1258.
- D'Imperio, L., Nielsen, C.S., Westergaard-Nielsen, A., Michelsen, A., Elberling, B., 2017. Methane oxidation in contrasting soil types: responses to experimental warming with implication for landscape-integrated CH<sub>4</sub> budget. *Glob. Chang. Biol.* 23, 966–976.
- Dooley, S.R., Treseder, K.K., 2012. The effect of fire on microbial biomass: a meta-analysis of field studies. *Biogeochemistry*. 109, 49–61.
- Dore, S., Kolb, T.E., Montes-Helu, M., Sullivan, B.W., Winslow, W.D., Hart, S.C., Kaye, J. P., Koch, G.W., Hungate, B.A., 2008. Long-term impact of a stand-replacing fire on ecosystem CO<sub>2</sub> exchange of a ponderosa pine forest. *Glob. Chang. Biol.* 14, 1801–1820.
- Evangelou, N., Kylling, A., Eckhardt, S., Myrioniuk, V., Stebel, K., Paugam, R., Zibtev, S., Stohl, A., 2019. Open fires in Greenland in summer 2017: transport, deposition and radiative effects of BC, OC and BrC emissions. *Atmos. Chem. Phys.* 19, 1393–1411.
- Fox, J., Weisberg, S., 2019. *An R companion to Applied Regression (Third)*. Sage, Thousand Oaks CA.
- Hermesdorf, L., Elberling, B., D'Imperio, L., Xu, W., Lambæk, A., Ambus, P.L., 2022. Effects of fire on CO(2), CH(4), and N(2) O exchange in a well-drained Arctic heath ecosystem. *Glob. Chang. Biol.* 28, 4882–4899.
- Hollingsworth, T.N., Johnstone, J.F., Bernhardt, E.L., Chapin 3rd, F.S., 2013. Fire severity filters regeneration traits to shape community assembly in Alaska's boreal forest. *PLoS. One* 8, e56033.
- Hu, F.S., Higuera, P.E., Duffy, P., Chipman, M.L., Rocha, A.V., Young, A.M., Kelly, R., Dietze, M.C., 2015. Arctic tundra fires: natural variability and responses to climate change. *Front. Ecol. Environ.* 13, 369–377.
- Hugelius, G., Strauss, J., Zubrzycki, S., Harden, J.W., Schuur, E., Ping, C.-L., Schirmer, L., Grosse, G., Michaelson, G.J., Koven, C.D., 2014. Improved estimates show large circumpolar stocks of permafrost carbon while quantifying substantial uncertainty ranges and identifying remaining data gaps. *Biogeosci.* 11, 4771–4822.
- Karhu, K., Dannenmann, M., Kitzler, B., Díaz-Pinés, E., Tejedor, J., Ramírez, D.A., Parra, A., Resco de Dios, V., Moreno, J.M., Rubio, A., Guimaraes-Povoas, L., Zechmeister-Boltenstern, S., Butterbach-Bahl, K., Ambus, P., 2015. Fire increases the risk of higher soil N<sub>2</sub>O emissions from Mediterranean *Macchia* ecosystems. *Soil Biol. Biochem.* 82, 44–51.
- Keeley, J.E., 2006. Fire severity and plant age in postfire resprouting of woody plants in sage scrub and chaparral. *Madroño* 53, 373–379.
- Keeley, J.E., 2009. Fire intensity, fire severity and burn severity: a brief review and suggested usage. *Int. J. Wildl. Fire* 18, 116–126.
- Kelly, J., Ibanez, T.S., Santin, C., Doerr, S.H., Nilsson, M.C., Holst, T., Lindroth, A., Kljun, N., 2021. Boreal forest soil carbon fluxes one year after a wildfire: effects of burn severity and management. *Glob. Chang. Biol.* 27, 4181–4195.
- Kennard, D.K., Gholz, H., 2001. Effects of high-and low-intensity fires on soil properties and plant growth in a Bolivian dry forest. *Plant Soil.* 234, 119–129.
- Klupar, I., Rocha, A.V., Rastetter, E.B., 2021. Alleviation of nutrient co-limitation induces regime shifts in post-fire community composition and productivity in Arctic tundra. *Glob. Chang. Biol.* 27, 3324–3335.
- Knicker, H., 2007. How does fire affect the nature and stability of soil organic nitrogen and carbon? A Review. *Biogeochem.* 85, 91–118.
- Koster, E., Koster, K., Berninger, F., Prokushkin, A., Aaltonen, H., Zhou, X., Pumpanen, J., 2018. Changes in fluxes of carbon dioxide and methane caused by fire in Siberian boreal forest with continuous permafrost. *J. Environ. Manage* 228, 405–415.
- Kulmala, L., Aaltonen, H., Berninger, F., Kieloaho, A.-J., Levula, J., Bäck, J., Hari, P., Kolari, P., Korhonen, J.F.J., Kulmala, M., Nikinmaa, E., Pihlatie, M., Vesala, T., Pumpanen, J., 2014. Changes in biogeochemistry and carbon fluxes in a boreal forest after the clear-cutting and partial burning of slash. *Agric. For. Meteorol.* 188, 33–44.
- Lewis, G., Osterberg, E., Hawley, R., Marshall, H.P., Meehan, T., Graeter, K., McCarthy, F., Overly, T., Thundercloud, Z., Ferris, D., 2019. Recent precipitation decrease across the western Greenland ice sheet percolation zone. *Cryosphere* 13, 2797–2815.
- Lombao, A., Barreiro, A., Fontúrbel, M., Martín, A., Carballas, T., Díaz-Raviña, M., 2020. Key factors controlling microbial community responses after a fire: importance of severity and recurrence. *Sci. Total Environ.* 741, 140363.
- Lu, S.-G., Sun, F.-F., Zong, Y.-T., 2014. Effect of rice husk biochar and coal fly ash on some physical properties of expansive clayey soil (Vertisol). *Catena (Amst)* 114, 37–44.

- Ludwig, S.M., Alexander, H.D., Kielland, K., Mann, P.J., Natali, S.M., Ruess, R.W., 2018. Fire severity effects on soil carbon and nutrients and microbial processes in a Siberian larch forest. *Glob. Chang. Biol.* 24, 5841–5852.
- Mack, M.C., Bret-Harte, M.S., Hollingsworth, T.N., Jandt, R.R., Schuur, E.A., Shaver, G.R., Verbyla, D.L., 2011. Carbon loss from an unprecedented Arctic tundra wildfire. *Nature* 475, 489–492.
- Mack, M.C., Treseder, K.K., Manies, K.L., Harden, J.W., Schuur, E.A.G., Vogel, J.G., Randerson, J.T., Chapin, F.S., 2008. Recovery of aboveground plant biomass and productivity after fire in mesic and dry black spruce forests of interior Alaska. *Ecosystems* 11, 209–225.
- McCarty, J.L., Aalto, J., Paunu, V.-V., Arnold, S.R., Eckhardt, S., Klimont, Z., Fain, J.J., Evangelidou, N., Venäläinen, A., Tchebakova, N.M., 2021. Reviews and syntheses: arctic fire regimes and emissions in the 21st century. *Biogeosciences* 18, 5053–5083.
- McCarty, J.L., Smith, T.E., Turetsky, M.R., 2020. Arctic fires re-emerging. *Nat. Geosci.* 13, 658–660.
- Montes-Helu, M., Kolb, T., Dore, S., Sullivan, B., Hart, S., Koch, G., Hungate, B., 2009. Persistent effects of fire-induced vegetation change on energy partitioning and evapotranspiration in ponderosa pine forests. *Agric. For. Meteorol.* 149, 491–500.
- Morishita, T., Noguchi, K., Kim, Y., Matsuura, Y., 2014. CO<sub>2</sub>, CH<sub>4</sub> and N<sub>2</sub>O fluxes of upland black spruce (*Picea mariana*) forest soils after forest fires of different intensity in interior Alaska. *Soil Sci. Plant Nutr.* 61, 98–105.
- Nowinski, N.S., Trumbore, S.E., Schuur, E.A., Mack, M.C., Shaver, G.R., 2008. Nutrient addition prompts rapid destabilization of organic matter in an arctic tundra ecosystem. *Ecosystems* 11, 16–25.
- Pereira, P., Francos, M., Brevik, E.C., Ubeda, X., Bogunovic, I., 2018. Post-fire soil management. *Curr. Opin. Environ. Sci. Health* 5, 26–32.
- Pereira, P., Ubeda, X., Martín, D.A., 2012. Fire severity effects on ash chemical composition and water-extractable elements. *Geoderma* 191, 105–114.
- Pluchon, N., Casetou, S.C., Kardol, P., Gundale, M.J., Nilsson, M.-C., Wardle, D.A., 2015. Influence of species identity and charring conditions on fire-derived charcoal traits. *Canad. J. For. Res.* 45, 1669–1675.
- Post, E., Alley, R.B., Christensen, T.R., Macias-Fauria, M., Forbes, B.C., Gooseff, M.N., Iler, A., Kerby, J.T., Laidre, K.L., Mann, M.E., 2019. The polar regions in a 2 C warmer world. *Sci. Adv.* 5, eaaw9883.
- Potter, C., Hugny, C., 2020. Wildfire effects on permafrost and soil moisture in spruce forests of interior Alaska. *J. For. Res. (Harbin)* 31, 553–563.
- Ravn, N.R., Elberling, B., Michelsen, A., 2020. Arctic soil carbon turnover controlled by experimental snow addition, summer warming and shrub removal. *Soil Biol. Biochem.* 142.
- Ribeiro-Kumara, C., Pumpanen, J., Heinonsalo, J., Metsläid, M., Orumaa, A., Jogiste, K., Berninger, F., Koster, K., 2020. Long-term effects of forest fires on soil greenhouse gas emissions and extracellular enzyme activities in a hemiboreal forest. *Sci. Total Environ.* 718, 135291.
- Rocha, A.V., Shaver, G.R., 2011a. Burn severity influences postfire CO<sub>2</sub> exchange in arctic tundra. *Ecol. Applic.* 21, 477–489.
- Rocha, A.V., Shaver, G.R., 2011b. Postfire energy exchange in arctic tundra: the importance and climatic implications of burn severity. *Glob. Chang. Biol.* 17, 2831–2841.
- Safdari, M.-S., Rahmati, M., Amini, E., Howarth, J.E., Berryhill, J.P., Dietsberger, M., Weise, D.R., Fletcher, T.H., 2018. Characterization of pyrolysis products from fast pyrolysis of live and dead vegetation native to the Southern United States. *Fuel* 229, 151–166.
- Schuur, T., McGuire, A.D., Romanovsky, V.E., Schadel, C., Mack, M., 2018. Arctic and boreal carbon.
- Stoof, C.R., Wesseling, J.G., Ritsema, C.J., 2010. Effects of fire and ash on soil water retention. *Geoderma* 159, 276–285.
- St Pierre, K.A., Danielsen, B.K., Hermesdorf, L., D'Imperio, L., Iversen, L.L., Elberling, B., 2019. Drivers of net methane uptake across Greenlandic dry heath tundra landscapes. *Soil Biol. Biochem.* 138.
- Takakai, F., Desyatkin, A.R., Lopez, C.M.L., Fedorov, A.N., Desyatkin, R.V., Hatano, R., 2010. Influence of forest disturbance on CO<sub>2</sub>, CH<sub>4</sub> and N<sub>2</sub>O fluxes from larch forest soil in the permafrost taiga region of eastern Siberia. *Soil Sci. Plant Nutr.* 54, 938–949.
- Talucci, A.C., Lorant, M.M., Alexander, H.D., 2022. Siberian taiga and tundra fire regimes from 2001 to 2020. *Environ. Res. Letters* 17, 025001.
- Team, R.C., 2021. Version 4.1. 2. R: a language and environment for statistical computing. R Foundation for Statistical Computing. Vienna: R Foundation for Statistical Computing.
- Thomas, A.D., Walsh, R.P., Shakesby, R.A., 2000. Post-fire forestry management and nutrient losses in eucalyptus and pine plantations. *North. Port. Land Degr. Dev.* 11, 257–271.
- Virkkala, A.-M., Virtanen, T., Lehtonen, A., Rinne, J., Luoto, M., 2018. The current state of CO<sub>2</sub> flux chamber studies in the Arctic tundra: a review. *Progr. Phy. Geogr.: Earth Environ.* 42, 162–184.
- Walker, X.J., Rogers, B.M., Veraverbeke, S., Johnstone, J.F., Baltzer, J.L., Barrett, K., Bourgeau-Chavez, L., Day, N.J., de Groot, W.J., Dieleman, C.M., Goetz, S., Hoy, E., Jenkins, L.K., Kane, E.S., Parisien, M.A., Potter, S., Schuur, E.A.G., Turetsky, M., Whitman, E., Mack, M.C., 2020. Fuel availability not fire weather controls boreal wildfire severity and carbon emissions. *Nat. Clim. Chang.* 10, 1130–1136.
- Woods, S.W., Balfour, V.N., 2008. The effect of ash on runoff and erosion after a severe forest wildfire, Montana, USA. *Int. J. Wildl. Fire* 17, 535–548.
- Woods, S.W., Balfour, V.N., 2010. The effects of soil texture and ash thickness on the post-fire hydrological response from ash-covered soils. *J. Hydrol.* 393, 274–286.
- Xu, W., Elberling, B., Ambus, P.L., 2022a. Fire increases soil nitrogen retention and alters nitrogen uptake patterns among dominant shrub species in an Arctic dry heath tundra. *Sci. Total Environ.* 807, 150990.
- Xu, W., Elberling, B., Ambus, P.L., 2022b. Pyrogenic organic matter as a nitrogen source to microbes and plants following fire in an Arctic heath tundra. *Soil Biol. Biochem.* 170.
- Xu, W., Elberling, B., Ambus, P.L., 2024. Long-term summer warming reduces post-fire carbon dioxide losses in an arctic heath tundra. *Agric. For. Meteorol.* 344, 109823.
- Xu, W., Lambæk, A., Holm, S.S., Furbo-Halken, A., Elberling, B., Ambus, P.L., 2021. Effects of experimental fire in combination with climate warming on greenhouse gas fluxes in Arctic tundra soils. *Sci. Total Environ.* 795, 148847.
- Zhou, L., Liu, S., Gu, Y., Wu, L., Hu, H.W., He, J.Z., 2023. Fire decreases soil respiration and its components in terrestrial ecosystems. *Funct. Ecol.*